# **Svalbard surface snowpack** Azzurra Spagnesi<sup>a,b</sup>, Elena Barbaro<sup>a,b</sup> \*, Matteo Feltracco<sup>a,b</sup>, Federico Scoto<sup>c,b</sup>, Marco Vecchiato<sup>b</sup>, Massimiliano Vardè<sup>a</sup>, Mauro Mazzola<sup>a</sup>, François Burgay<sup>d,e</sup>, Federica Bruschi<sup>f</sup>, Clara Jule Marie Hoppe<sup>g</sup>, Allison Bailey<sup>g</sup>, Andrea Gambaro<sup>a,b</sup>, Carlo Barbante<sup>a,b</sup>, Andrea Spolaor<sup>a,b</sup> <sup>a</sup> Institute of Polar Sciences - National Research Council of Italy (ISP-CNR), Via Torino 155, 30172, Venice, Italy <sup>b</sup> Department of Environmental Sciences, Informatics and Statistics, Ca' Foscari University of Venice, Via Torino 155, 30172, Venice, Italy <sup>c</sup> Institute of Atmospheric Sciences and Climate - National Research Council of Italy (ISAC-CNR), Campus Ecotekne, Lecce, 73100, Italy <sup>d</sup> Laboratory of Environmental Chemistry (LUC), Paul Scherrer Institut (PSI), Villigen, 5232, Switzerland <sup>e</sup> Oeschger Centre for Climate Change Research, University of Bern, Bern, 3012, Switzerland <sup>f</sup> Department of Chemistry, Biology and Biotechnology, University of Perugia, Via dell'Elce di Sotto 8, 06123, Perugia, g Alfred Wegener Institute, Helmholtz Centre for Polar and Marine Research, 27570 Bremerhaven, Germany Corresponding: Elena Barbaro (elena.barbaro@cnr.it)

Seasonal and interannual variability on the chemical composition of the

#### Abstract

Arctic Amplification (AA) is driving long-term changes in the Arctic climate system, including glacier ice melt, rapid sea ice decline, and alterations in atmospheric and geochemical processes, with consequences on the formation, transport, and chemical composition of aerosols and seasonal snowpack. Svalbard, particularly vulnerable to AA, provides a valuable site to assess changes in local environmental processes contributing to the seasonal snow chemical composition. From 2018 to 2021, sampling campaigns at the Gruvebadet Snow Research Site in Ny-Ålesund, in the North-West of the Svalbard Archipelago, captured the interannual variability in ionic and elemental impurities within surface snow, reflecting seasonal differences in atmospheric and oceanic conditions. Notably, warmer conditions prevailed in 2018-19 and 2020-21, contrasting with the relatively colder season of 2019-20. Our findings suggest that impurity concentrations in the 2019-20 colder season are impacted by enhanced sea spray aerosol production, likely driven by a larger extent of sea ice, and drier, windy conditions. This phenomenon was particularly evident in March 2020, when extensive sea ice was present in Kongsfjorden and around Spitsbergen due to an exceptionally strong, cold stratospheric polar vortex and unusual Arctic Oscillation (AO) index positive phase. By comparing the snow chemical composition of the 2019-20 season with 2018-19 and 2020-21, we provide insights into the interplay between short-term meteorological variability and the long-term climatic impacts of AA in Svalbard, as well as associated shifts in aerosol production process.

## 1. Introduction

Chemical analysis of surface Arctic snow and ice can provide valuable comprehension of the composition of Arctic aerosols, its deposition, and exchange processes (Lai et al., 2017). These processes are influenced by a range of factors, including Arctic Amplification (AA) – a pronounced, long-term increase in near-surface air temperature observed since 1975 (Chylek et al., 2022). AA is recognized as an inherent characteristic of the global climate system, with multiple intertwined causes operating on a spectrum of spatial and temporal scales. These include, but are not limited to, changes in sea ice extent that impact heat fluxes between the ocean and the atmosphere, and water vapor that alters longwave radiation (Serreze and Barry, 2011). The Svalbard Archipelago is particularly sensitive to these effects due to the relatively low altitude of its main ice fields and its geographical location in the higher North Atlantic, where the impact of AA is especially pronounced (Spolaor et al., 2024). Therefore, in the 21<sup>st</sup> century, predicting and characterizing climate change in Svalbard is particularly crucial, as changes in near-surface air temperature, precipitation, and sea ice extent occur at an extremely high pace (Gjermundsen et al., 2020; Rantanen et al., 2022). The Svalbard region,

located at the southern edge of the seasonal Arctic sea-ice zone, is characterized by a maritime climate 63 with strong temperature variations during winter (Hansen et al., 2014; Barbaro et al., 2021). In the 64 Arctic winter, the stratospheric polar jet fosters a high-atmospheric vorticity zone. This winter vortex 65 typically acts as a strong barrier for the long-range transport of pollutants from mid-latitudes 66 (Lawrence et al., 2020). However, it occasionally allows warm southern air to penetrate the region 67 (Schoeberl and Newman, 2015). Additionally, Svalbard frequently experiences intense cyclonic 68 69 storms in autumn and winter, which bring both heat and moisture from lower latitudes (Rinke et al., 70 2017). These intense meteorological variations, generally linked with a weaker polar vortex (Sobota 71 et al., 2020; Salzano et al., 2023), favor long-range transport of aerosols to the archipelago, including pollutants from continental sources (Stohl et al., 2006b; Yttri et al., 2014a; Vecchiato et al., 2024; 72 73 D'Amico et al., 2024).

Arctic snow captures dry and wet deposition and forms an archive that includes a range of seasonal 74 chemical species such as major ions and trace elements, as well as human-made pollutants emitted 75 into the Arctic atmosphere (Koziol et al., 2021). Ny-Ålesund is a well-monitored area and a natural 76 77 laboratory for complex system observations, ideal for exploring both long-range contaminants from mid- to high-latitude regions of Eurasia and Canada (Nawrot et al., 2016; Song et al., 2020; Vecchiato 78 79 et al., 2024; D'Amico et al., 2024), and local inputs from both natural processes and human settlement 80 (Vecchiato et al., 2018). Previous research has extensively investigated the chemistry of Arctic snow and the exchange of inorganic species between the cryosphere and the atmosphere across multiple 81 82 sites, including Barrow, Summit Greenland, Alert, Sodankylä, and over the Arctic Ocean during the 83 MOSAiC expedition (e.g., Beine et al., 2003; Björkman et al., 2013; Jacobi et al., 2019). Specific studies in Ny-Ålesund and surrounding areas have explored the temporal and compositional aspects 84 85 of the lower atmosphere (Stohl et al., 2006a; Eleftheriadis et al., 2009; Geng et al., 2010; Zhan et al., 2014; Feltracco et al., 2020, 2021; Turetta et al., 2021), though relatively few have addressed the 86 87 detailed seasonal dynamics of snow-atmosphere interactions in this region. Building on this existing research, our study aims to enhance the understanding of these interactions, particularly in the context 88 89 of recent climatic changes.

In this study, we evaluate the surface snow concentration of ionic (Cl<sup>-</sup>, Br<sup>-</sup>, NO<sub>3</sub><sup>-</sup>, SO<sub>4</sub><sup>2</sup>-, MSA, Na<sup>+</sup>, 90 NH<sub>4</sub><sup>+</sup>, K<sup>+</sup>, Ca<sup>2+</sup>) and elemental impurities (Li, Be, Mg, Al, Ca, V, Cr, Mn, Fe, Co, Ni, Cu, Zn, As, Se, 91 Rb, Sr, Ag, Cd, Sb, Cs, Ba, Tl, Pb, Bi, U) for the snow seasons between 2018-2021, at the Gruvebadet 92 Snow Research Site (GSRS) location, 1 km south of Ny-Ålesund, where clean and undisturbed snow 93 94 conditions are guaranteed throughout the whole sampling season. The differences in average meteorological and climatological conditions across the studied seasons 95

are analysed to assess how sea ice extent, polar vortex, and Arctic Oscillation (AO) conditions influence the composition of surface snow in connection with the aerosol-producing and deposition processes in Kongsfjorden.

#### 2. Methodology

96

97

98

99

100

127

128

2.1 Sampling and processing

Three sampling campaigns were conducted in Svalbard between 2018 and 2021, covering the period 101 from October to May according to the onset of the snowpack formation and melting. Sample 102 collection followed the protocol presented in Spolaor et al. (2019), further adopted by Bertò et al. 103 (2021), where consecutive and adjacent sampling was carried in a 3x3 meters snow sampling area, 104 105 within a clean sampling snowfield of 100 m wide. Each sample was collected 10 cm apart from the previous one, along a precise path. This method was designed to minimise the temporal variability 106 107 between consecutive samples and reduce the impact of potential spatial variability (within the 5-15% 108 range, according to Spolaor et al., 2019). During the first sampling campaign, carried out from October 4<sup>th</sup>, 2018 to May 10<sup>th</sup>, 2019, 114 surface 109 snow samples were collected in a delimited snow field located ~ 100 m south of the "Dirigibile Italia 110 Station" in Ny-Ålesund (78.92° N 11.93° E, Ny-Ålesund, Svalbard). The surface snow was sampled 111 within the upper 3 cm, as this is the snow layer most influenced by the aerosol-cryosphere exchanges, 112 and, in case of snowfall, by deposition (Spolaor et al., 2018, 2021b). This choice also minimised the 113 effect of different physical snow conditions (density, crystal shape, and size). 114 Concurrently, additional 133 snow samples were collected at the Gruvebadet Snow Research Site 115 (GSRS) to evaluate the spatial variability with respect to the snow samples collected in Ny-Ålesund. 116 The GSRS is a clean-area located about 1 km south of Ny-Ålesund, nearby the Gruvebadet 117 Atmospheric Laboratory (GAL), dedicated to the chemical and physical monitoring of the seasonal 118 snowpack (Scoto et al., 2023; Fig. S1). Throughout the season, the sampling resolution varied based 119 on light conditions. During the polar night (from October to early March), snow sampling was carried 120 out daily at Ny-Ålesund, and every 3-5 days at the GSRS. With the beginning of the polar day, daily 121 sampling was conducted both in Ny-Ålesund and at the GSRS in March, and then continued only at 122 the GSRS until the end of the snow season in June due to the lower contamination of the site, more 123 distant from the fervent local activities. This sampling resolution overlap during March ensured a 124 good comparison of results in both snow fields (Fig. S2). 125 Starting from the second campaign, snow sampling activities were conducted only at the GSRS site, 126 since clean conditions of the field in Ny-Ålesund could not be guaranteed due to construction works.

- samples collected. The surface snow layer was sampled every 3-5 days during the polar night (until
- February 24<sup>th</sup>, 2020), and daily from the beginning of the polar day until the end of the snow season.
- 131 Consecutive samples represent the same snow layer in the absence of snowfall or wind drift/erosion.
- However, factors such as snow aging, potential element re-emission, transformation, and dry
- deposition can introduce variability, making continuous monitoring essential.
- Finally, during the third snow sampling campaign, lasting from October 27<sup>th</sup>, 2020 to June 15<sup>th</sup>, 2021,
- a weekly sampling was conducted at GSRS, with a total of 32 samples collected.
- During snow sampling, the temperature and density of surface snow were measured, and the density
- of snow was calculated based on weighting a 100 cc cylinder. After collection, snow samples were
- melted, and two different aliquots were obtained and stored in separate vials. In a 1.5 mL
- polypropylene (PP) vial, 1 mL of sample was stored for ionic species, while another aliquot was
- stored in a 5 mL LDPE vials for trace elements analysis. PP vials designated to ionic species analysis
- were previously sonicated for 30 min in UltraPure Water (UPW) (18 MΩ cm<sup>-1</sup> at 25 °C) for
- decontamination. LDPE vial used for trace elements analysis were instead conditioned with HNO<sub>3</sub>
- 2% and sonicated for 30 min. All sample aliquots were stored at -20°C in dark conditions and
- transported to the Venice ISP-CNR laboratories.
- Furthermore, seawater temperatures and salinity at 10 m depth were also monitored in Kongsfjorden
- 146 (Kb3; 78°57.228'N, 11°57.192'E) during 2019-2021 spring seasons, with data collected every 3-6
- days (Assmy et al. 2023). Data was derived from Conductivity Temperature Depth (CTD) casts with
- either a MiniSTD model SD-204 (SAIV A/S, Bergen, Norway) or a XR-620 CTD (RBR Ltd, Ottawa,
- 149 Canada). Combined casts of both instruments conducted in May 2020 and 2021 did not reveal
- differences in temperature or salinity in the reported accuracy (two post comma digits).

## 2.2 Analysis of ionic species

- The analysis of anionic species (Cl<sup>-</sup>, Br<sup>-</sup>, NO<sub>3</sub><sup>-</sup>, SO<sub>4</sub><sup>2</sup>-, MSA) was carried out using an ion
- chromatograph (IC, Thermo Scientific Dionex<sup>TM</sup> ICS-5000, Waltham, MA, USA) coupled with a
- single quadrupole mass spectrometer (MS, MSQ Plus<sup>TM</sup>, Thermo Scientific, Bremen, Germany). The
- separation was performed using an anionic exchange column (Dionex Ion Pac AS 19 2 mm ID  $\times$  250
- mm length) equipped with a guard column (Dionex Ion Pac AG19 2 mm ID × 50 mm length). Sodium
- hydroxide (NaOH), used as mobile phase, was produced by an eluent generator (Dionex ICS 5000EG,
- 158 Thermo Scientific). The NaOH gradient with a 0.25 mL min<sup>-1</sup> flow rate was: 0-6 min at 15 mM; 6-
- 159 15 min gradient from 15 to 45 mM; 15-23 min column cleaning with 45 mM; 23–33 min equilibration
- at 15 mM. The injection volume was 100 µL. A suppressor (ASRS 500, 2 mm, Thermo Scientific)
- removed NaOH before entering the MS source. The IC-MS operated with a negative electrospray

- source (ESI) with a temperature of 500°C and a needle voltage of 3 kV. The other MS parameters are
- reported by Barbaro et al. (2017). The same IC system was simultaneously used to determine cationic
- species (Na<sup>+</sup>, K<sup>+</sup>, Ca<sup>2+</sup> and NH<sub>4</sub><sup>+</sup>). However, Ca<sup>2+</sup> was not measured within the samples collected
- during the second campaign due to instrumental limitations.
- The separation occurred with a capillary cation-exchange column (Dionex Ion Pac CS19–4 mm 0.4
- mm ID  $\times$  250 mm length), equipped with a guard column (Dionex Ion Pac CG19–4, 0.4 mm ID  $\times$  50
- 168 mm length), and the species were determined using a conductivity detector. Analytical blanks of
- ultrapure water (>  $18 \text{ M}\Omega \text{ cm}$ ) were included in the analysis, and the Method Detection Limit (MDL)
- was set to 3 times the standard deviation of the blank values. Checks for accuracy were made using
- 171 certified multi-element standard solutions for anions (Cl<sup>-</sup>, Br<sup>-</sup>, NO<sub>3</sub><sup>-</sup>, SO<sub>4</sub><sup>2-</sup>, no. 89886-50ML-F, Sigma
- Aldrich) and cations (Na<sup>+</sup>, K<sup>+</sup>, Ca<sup>2+</sup>, no. 89316-50ML-F, Sigma Aldrich) at a concentration of 10 mg
- 173  $L^{-1} \pm 0.2\%$ . The analytical precision was quantified as the relative standard deviation (RSD) for
- replicates (n > 3) of standard solutions and was always < 10% for each ion.

### 2.3 Trace Elements analysis

- 176 Twenty-six elements (Li, Be, Mg, Al, Ca, V, Cr, Mn, Fe, Co, Ni, Cu, Zn, As, Se, Rb, Sr, Ag, Cd, Sb,
- 177 Cs, Ba, Tl, Pb, Bi and U) were analyzed on samples previously melted and acidified to 2% v/v with
- HNO<sub>3</sub> (UpA grade, Romil, UK) for 24 hours before analysis (Spolaor et al., 2018; Spolaor et al.,
- 179 2021a).

175

- The analysis was performed using Inductively Coupled Plasma Mass Spectrometry (ICP-MS, iCAP)
- 181 RQ, Thermo Scientific, US). The ICP-MS was equipped with an ASX-560 autosampler (Teledyne
- 182 Cetac Technologies), PolyPro PFE nebulizer, PFE cyclonic spray chamber thermostated at 2.7°C,
- sapphire injector, quartz torch and Ni cones. The acquisition was performed at 1550 W of plasma RF
- power in Kinetic Energy Discrimination (KED) high matrix mode, using He as collision gas (4.3
- 185 mL min<sup>-1</sup>). Instrument parameters were optimized for best sensitivity in the whole mass range,
- minimum oxides (< 1%) and double charges (< 3%). Quantification was obtained by external
- calibration with multi-elemental standards prepared in ultrapure water (18 M $\Omega$  cm<sup>-1</sup> at 25° C) with
- 2% v/v ultrapure grade HNO<sub>3</sub> (UpA grade, Romil, UK), with a combination of certified level multi-
- elemental solutions IMS-102 and IMS-104 from UltraScientific. Analytical quality control was
- performed by memory test blank (repeated analysis of ultrapure grade HNO<sub>3</sub> 2% v/v blank solution)
- after each sample and calibration verification (repeated analysis of reference standards) every 11
- samples. More details are found in Spolaor et al., 2021a.

193

The Lagrangian particle dispersion model HYSPLIT (Draxler, 1998; Stein et al., 2015) was used to determine the source region of air masses over Ny-Ålesund. This model has previously been shown to be an effective tool for the prediction of transport pathways into and within the Arctic and Antarctic regions (Barbaro et al., 2015; Feltracco et al., 2021). The simulations were driven using meteorological data from the Global Data Assimilation System (GDAS) one-degree archive, set the top of the model at 10000 m and the height source equal to the GSRS altitude. Back-trajectories were calculated every 6 h, with a propagation time of 120 h for each sampling period, as suggested in previous studies on atmospheric circulation in the same site (Feltracco et al., 2021). This approach was used to ensure an envelope working for all investigated tracers. The resulting multiple trajectories were based on the screen-plot analyses of total spatial variance.

The Ice Service provided by the Norwegian Meteorological Institute (NIS) was employed to analyse the weather conditions via remotely sensed data and to generate ice charts of Svalbard, ice-edge information, and sea surface temperatures trends. Sea ice extent variability in Kongsfjorden was evaluated based on dataset made available by Gerland et al. (2022).

Differences between the sampling campaigns were evaluated through the NCEP/NCAR Reanalysis data from NOAA Physical Sciences Lab's daily composites tool, used to calculate the near-surface air temperatures across the Northern Hemisphere from October to May.

#### 2.5 Statistical procedures and Enrichment Factors (EFs) Analysis

Results below the limit of detection were assumed to be equal to ½ of Method Determination Limit (MDL) prior to perform statistical analysis, to approximate their likely level based on the data distribution curve (best approximated as log-normal for most of the studied variables) (George et al., 2021).

The Wilcoxon test was applied on data from the 2018-19 sampling campaign conducted at Ny-Ålesund and Gruvebadet to determine whether the difference between the population median and the

The Wilcoxon test was applied on data from the 2018-19 sampling campaign conducted at Ny-Ålesund and Gruvebadet to determine whether the difference between the population median and the hypothesized median of surface snow contamination level was statistically significant. This model assumes that the data is sampled from two matched or dependent populations, and data is assumed to be continuous. Because it is a nonparametric test, it does not require a particular probability distribution of the dependent variable in the analysis. Furthermore, Enrichment Factors (EFs) using Ba as a crustal element of reference (Widepohl, 1995; Spolaor et al., 2021a; Ruppel et al., 2023), were calculated to explore the mixed sources of the investigated elements. To complement the EFs analysis, a Hierarchical Cluster Analysis (HCA) was performed using Ward's algorithm and

Euclidean distances as clustering criteria, to determine the presence of some clusters and simplify the interpretation of the dataset.

231

232

233

234

235

236

237

238

239

240

241

242

243

244

245

246

247

248

249

250

251

252

253

254

255

256

257

258

thickness of sampled strata.

229

230

#### 3 Results

## 3.1 Comparison between concentration trends at Gruvebadet and Ny-Ålesund

The concentration variations between an undisturbed area in Ny-Ålesund village and GSRS sites were compared during the 2018-19 sampling campaign to better understand the effect of spatial variability between the two sampling sites. The concentration trends of Na+, as sea salt tracer, Pb as anthropogenic species, and Ca<sup>2+</sup> as crustal tracer, are reported in Fig. S2, for both sampling sites. Although the difference in time resolution between sites is apparent in Fig. S2, the difference in concentration trends appears very low or negligible, except for sporadic peaks in sea salt and crustal tracers present in the Ny-Ålesund record from November to February. These peaks do not consistently correlate with positive temperature anomalies and precipitation events, as some occurred under low temperatures and without significant precipitation (e.g., January and early February), suggesting that other processes, such as long-range transport, wind-driven deposition, or dry deposition may also play a role (Fig. S2). Concordant Pb trends emerge at Ny-Ålesund and Gruvebadet, with the highest concentrations observed from February to May. To evaluate the differences in concentration range and spatial distribution of surface snow impurity content, we applied the Wilcoxon test for the 2018-19 sampling period by comparing the distributions for positive and negative differences of the ranks of their absolute values. At a significance level of 0.01, the two distributions from GSRS and Ny-Ålesund sites were not statistically different for all the trace elements and most of the inspected ions. For this reason, only the GSRS temporal trend has been considered throughout the manuscript, referring to ionic loads (mg m<sup>-2</sup>) instead of concentrations (ng g<sup>-1</sup>), to highlight the seasonal trends of specific tracers. The ionic load is calculated as ionic concentrations multiplied by the density and the

## 3.2 Interannual trends of chemical species on the surface snow

Three consecutive snow seasons were evaluated to define the chemical composition of the surface snow in the Arctic site of GSRS. The sea salt ions  $Cl^{-}(50 \%)$ ,  $Na^{+}(23\%)$  represent the most abundant species, followed by  $SO_4^{2-}(11 \%)$ , Mg (7 %), Ca (2%), Fe (1%) and Al (1%). Similar relative

abundances were also found in previous studies on the snow of the Svalbard Archipelago (Beaudon and Moore, 2009; Vega et al., 2015; Barbaro et al., 2021; Spolaor et al., 2021b).

Table 1 reports the average ionic loads of the most abundant (> 1%) species in the surface snow, considering three different seasons: autumn is defined until December 21<sup>st</sup>, winter until March 21<sup>st</sup>, and spring from then to the melt onset, identified by 5-6 consecutive days of negative snow accumulation. The average ionic loads of the less abundant (< 1%) species are reported instead in Table S1.

**Table 1.** Average ionic loads of the most abundant (>1%) ionic and elemental species in the surface snow during each season of the three consecutive sampling campaigns. The standard deviation is shown in brackets, while in the case of  $nss-SO_4^{2-}$  the brackets represent the percentage of  $nss-SO_4^{2-}$  compared to the total  $SO_4^{2-}$ . "n" indicates the number of samples considered for the calculation of the average.

2	7	0
2	7	1

mg m <sup>-2</sup>	total	Cl <sup>-</sup>	Na <sup>+</sup>	SO <sub>4</sub> <sup>2</sup> -	nss-SO <sub>4</sub> <sup>2-</sup>	Mg	Fe	Ca	NO <sub>3</sub> -	<b>K</b> <sup>+</sup>	NH <sub>4</sub> <sup>+</sup>
autumn 2018 (n=22)	32	15	7	3	1	3	2	0.3	0.5	0.3	0.04
	(25)	(21)	(11)	(4)	(36%)	(3)	(5)	(0.3)	(0.5)	(0.4)	(0.03)
winter 2018-19 (n=41)	116	55	31	16	8	8	0.4	0.4	2	2	0.3
	(80)	(68)	(39)	(16)	(51%)	(8)	(0.3)	(0.3)	(2)	(2)	(0.3)
spring 2019 (n=51)	76	36	19	9	4	6	2	0.6	1	1	0.5
	(50)	(43)	(24)	(9)	(48%)	(5)	(3)	(0.4)	(1)	(1)	(0.4)
autumn 2019 (n=15)	214	101	40	26	16	10	1	9	5	2	4
	(98)	(71)	(53)	(20)	(61%)	(6)	(1)	(12)	(4)	(3)	(5)
winter 2019-20 (n=43)	339	159	79	41	21	16	2	9	3	3	7
	(120)	(88)	(73)	(20)	(52%)	(8)	(5)	(10)	(2)	(4)	(8)
spring 2020 (n=49)	273	110	52	28	15	21	6	13	4	2	5
	(132)	(91)	(77)	(25)	(53%)	(21)	(9)	(16)	(2)	(4)	(8)
autumn 2020 (n=6)	803	435	191	66	18	84	1	2	6	9	2
	(542)	(466)	(205)	(83)	(27%)	(165)	(2)	(5)	(11)	(10)	(2)
winter 2020-21 (n=13)	327	207	64	41	24	6	0.2	0.2	5	3	1
	(203)	(194)	(48)	(36)	(60%)	(5)	(0.4)	(0.1)	(3)	(2)	(1)
spring 2021 (n=13)	181	107	36	16	7	9	4	1	3	2	1
	(92)	(86)	(26)	(12)	(43%)	(10)	(7)	(2)	(2)	(2)	(1)

The average loads of the first sampling year were lower compared to the other campaigns (Fig. S3). High average loads were observed instead for Cl<sup>-</sup> and Na<sup>+</sup> in the top snowpack layer during the 2019-20 and 2020-21 winter seasons. The highest concentrations of sea salt species were found in autumn 2020 (Fig. 1), despite low snow accumulation in a period of relatively high precipitation (Table S3). This apparent contradiction can likely be attributed to the increased wind speeds during that time, which may have caused snow redistribution, thereby limiting accumulation despite the considerable precipitation.

The non-sea-salt sulphate (nss- $SO_4^{2-}$ ), calculated using a seawater  $SO_4^{2-}/Na^+$  mass ratio of 0.252 (Millero et al., 2008), was the most abundant fraction of the total sulphate in autumn 2019 and winter 2020-21, while in autumn 2018 and 2020 sea salt sulphate (ss- $SO_4^{2-}$ ) was the dominant fraction. No

clear predominance between the two fractions was achieved during the other investigated seasons (Table 1).

The abundance of all chemical species investigated is quite similar for all years (Fig. S3), although the sampling campaign 2019-20 showed higher percentage of calcium ranging between 3% and 5%, in contrast to the typical concentrations < 1% found in the other two campaigns.

#### 3.3 Polar vortex and Arctic Sea ice extent in 2019-20

According to the 2023 survey conducted by the National Snow and Ice Data Center (NSIDC), the maximum extent of Arctic Sea ice since 2014 has been recorded in March 2020, with 14.73 million square kilometres of the Arctic Ocean surface, in a decadal trend characterized by a -2.53% of decline, due to the Arctic Amplification. Considering the Kongsfjorden area, the total sea ice extent varied from 63.94 km<sup>2</sup> in March 2019 to 129.81 km<sup>2</sup> in March 2020, and was with 46.26 km<sup>2</sup> lowest in March 2021 (Gerland et al., 2022). Specifications on Drift Ice (DI), Fast Ice (FI), and Open Water (OW) extent are reported in Table S2. The 2020 maximum sea ice extent followed the exceptionally strong and cold stratospheric polar vortex that took place in the Northern Hemisphere (NH) during the 2019-20 polar winter, together with low wave activity from the troposphere, which allowed the polar vortex to remain relatively undisturbed (Lawrence et al., 2020). Notably, the 2020 Arctic Sea ice extent is 16% and 9% higher than previous (2018-19) and following (2020-21) records (dataset NSIDC, NOAA). Lower surface air temperatures, reduced precipitations, higher wind speed (m sec-1), and minor mean snow height were observed during the 2019-20 winter season, attributed to the influence of a strong polar vortex triggered by a net positive Artic Oscillation (AO) phase. The 2020 anomalous AO index is displayed in Fig. S4. Seasonal values of mean air temperatures (°C), mean precipitation (mm), maximum mean wind speed (m sec<sup>-1</sup>) and mean snow depth (cm) during the three consecutive sampling campaigns are reported in Table S3. Temperature data were provided by the Norwegian Centre for Climate Services (NCCS), while sea ice extent data were supplied by National Snow and Ice Data Center (NSIDC). Seawater temperature data collected at 10 m depth at a midfjord station near Ny-Ålesund (Kb3) was found to be colder during 2020 compared to 2019 and 2021 spring seasons (Table S4). Although these temperatures were still above the freezing point for the observed salinity levels, they contributed to colder overall conditions in Kongsfjorden, supporting the formation and prolonged presence of sea ice when combined with cold atmospheric conditions.

#### 4. Discussion

285

286

287

288

289

290

291

292

293

294

295

296

297

298

299

300

301

302

303

304

305

306

307

308

309

310

311

312

313

4.1 Ny-Ålesund seasonal and interannual trends variability in surface snow

The three consecutive sampling campaigns conducted from 2018 to 2021 confirmed the dominance of sea salt input in the surface snow of Svalbard, due to the proximity of the Kongsfjord (Barbaro et al., 2021). The dominant ions are Na<sup>+</sup>, Cl<sup>-</sup>, and SO<sub>4</sub><sup>2-</sup>, associated with the scavenging precipitation of marine aerosol (Hodgkins and Tranter, 1998). The observed mean seasonal trends (Fig. S3) display the highest concentrations of marine species in autumn 2020, followed by 2020-21 and 2019-20 winter seasons. However, wintry concentrations are presumably linked to weakened (2019-20) or destroyed (2020-21) polar vortex (Fig. 1) and intense cyclonic storms, associated with anomalous warming events capable of transporting both heat and moisture from lower latitudes to Svalbard (Rinke et al., 2017). In addition to these factors, it is important to account for snow ablation or erosion by wind. The change in snow height (Δh) between consecutive sampling events provides valuable insights into such processes. A decrease in snow height signals ablation can indeed result from snow melting (under positive temperatures), snow aging, sublimation, or snow drift. In particular, when wind speeds exceed 5 m s<sup>-1</sup>, the threshold commonly accepted for initiating snow drift and ablation episodes (Pomeroy, 1989), we can infer the snow erosion due to wind drift likely occurred (Fig. 1). This effect may explain some of the variability in snow ion concentrations, especially during intense storms or strong winds.

Autumn 2020 represents most likely an outlier, due to scarce precipitations (Fig. 2) that led to more concentrated impurities in the surface snow. Meanwhile, late spring 2020 saw a notable increase of typical marine ions (Na<sup>+</sup>, Cl<sup>+</sup>, Br-, MSA, SO4<sup>2-</sup>) and geogenic elements (Al, Ca, Mn, Fe, Sr), compared to spring 2019 (Fig. 2). This increase may be attributed to the very close drift Arctic Sea ice presence in Kongsfjorden (Table S2), which reached its maximum extent in March 2020 due to low-temperature anomalies and intensified atmospherically driven sea ice transport and deformation due to higher winter wind speeds (Fig. S5). These conditions likely enhanced the production of sea spray aerosols, which, when carried by winds, may have increased the deposition of marine species onto the snowpack. Such atmospheric and environmental factors appear to have significantly contributed to the observed peaks of marine and geogenic species during this period. Concurrently, an outstanding positive phase of the Arctic Oscillation (AO) in the troposphere (Fig. 1) was recorded in January-March 2020 (Lawrence et al., 2020; Dethloff et al., 2022). Although the entire period was remarkable, January and February featured as clear outliers in the historical timeseries (1950–2023) reported by the NOAA service, while March 2020 exhibited significantly elevated values but did not exceed the statistical threshold for outliers (Fig. S4).

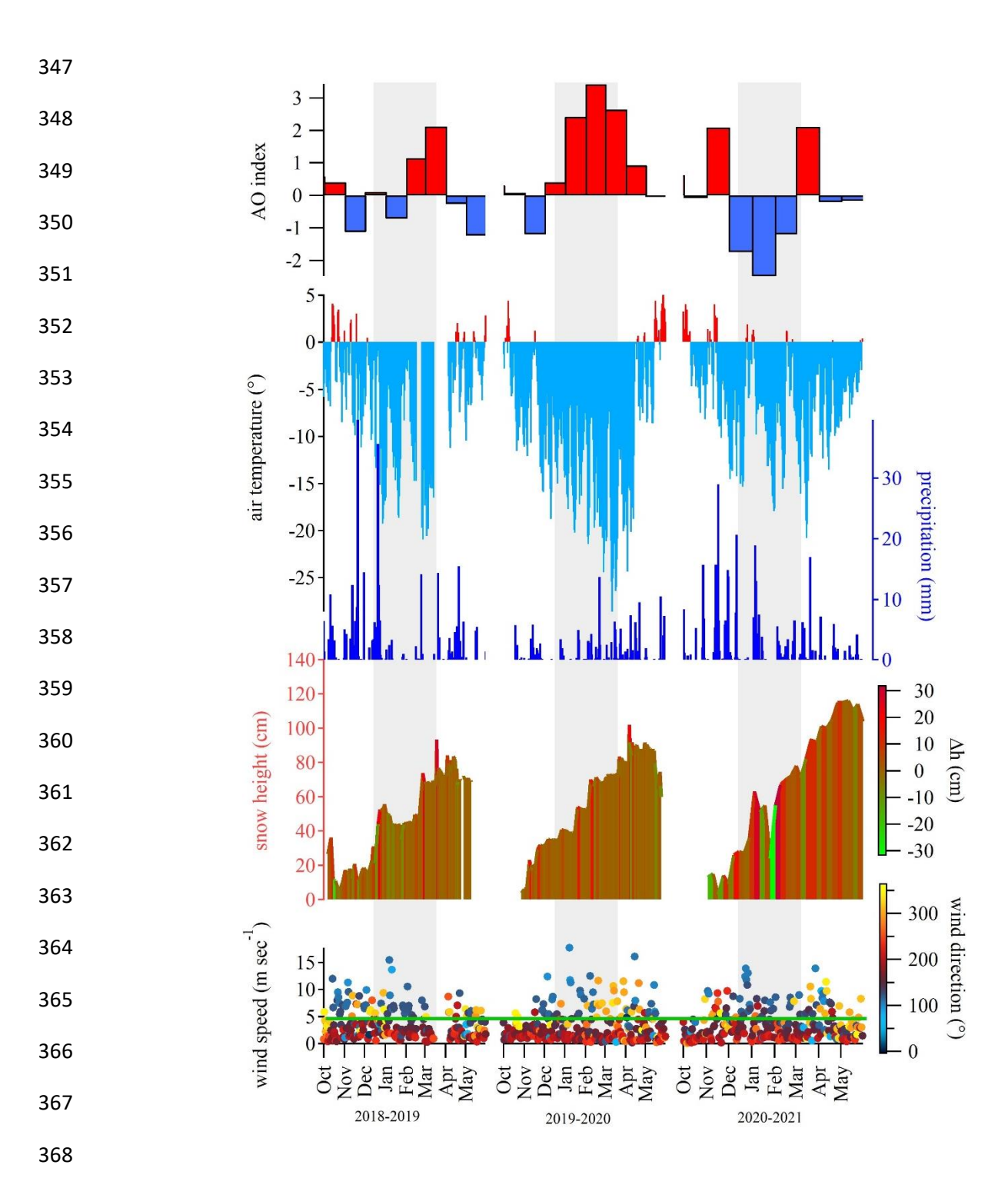


**Figure 1.** AO Index, air temperature (°C), precipitation (mm), snow height (cm),  $\Delta h$  snow height (cm), wind speed (m sec<sup>-1</sup>), and wind direction (°) from the NCEP/NCAR Reanalysis data. The green horizontal line above the wind speed graph indicates the 5 m sec<sup>-1</sup> threshold, above which wind drift may occur on surface snow layers. The colour of the line refers to the  $\Delta h$  color scale, which indicates negative values of  $\Delta h$ , NOAA Physical Sciences Lab's daily composites tool was used to calculate the near-surface air temperatures across the Northern Hemisphere from October to May. Grey bands indicate the winter periods.

A 2021 spring peak of marine species was also recorded, although more attenuated than in spring 2020 (Fig. 2, Fig. S3). This variation is likely attributable to different extents of sea ice in the fjord. Nonetheless, seawater temperatures in 2021, similar to those in 2020 and 2.3°C colder than in 2019 (Table S4), along with comparable wind speed conditions (Fig. S5), may also have contributed to the observed trends in marine species concentrations. Similarly, the spring peak of Mg, Sr, Mn, Fe, Al, and V in 2021 seems to reflect the high wind speed and positive AO index recorded from March to April 2021. Positive anomalies for air temperatures (A) and wind speed (W) conditions, together with negative anomalies in seawater (O) conditions were observed during the 2020-21 campaign, while negative A and O conditions were accompanied to positive W during 2019-20. On the contrary, 2018-19 diverges from the other campaigns for positive O condition associated to negative W condition anomalies. These observations provide valuable insights into how shifts in atmospheric and oceanic conditions impact the concentrations of ionic and elemental species in surface snow, enhancing our understanding of the underlying mechanisms that govern these changes in the context of AA conditions.

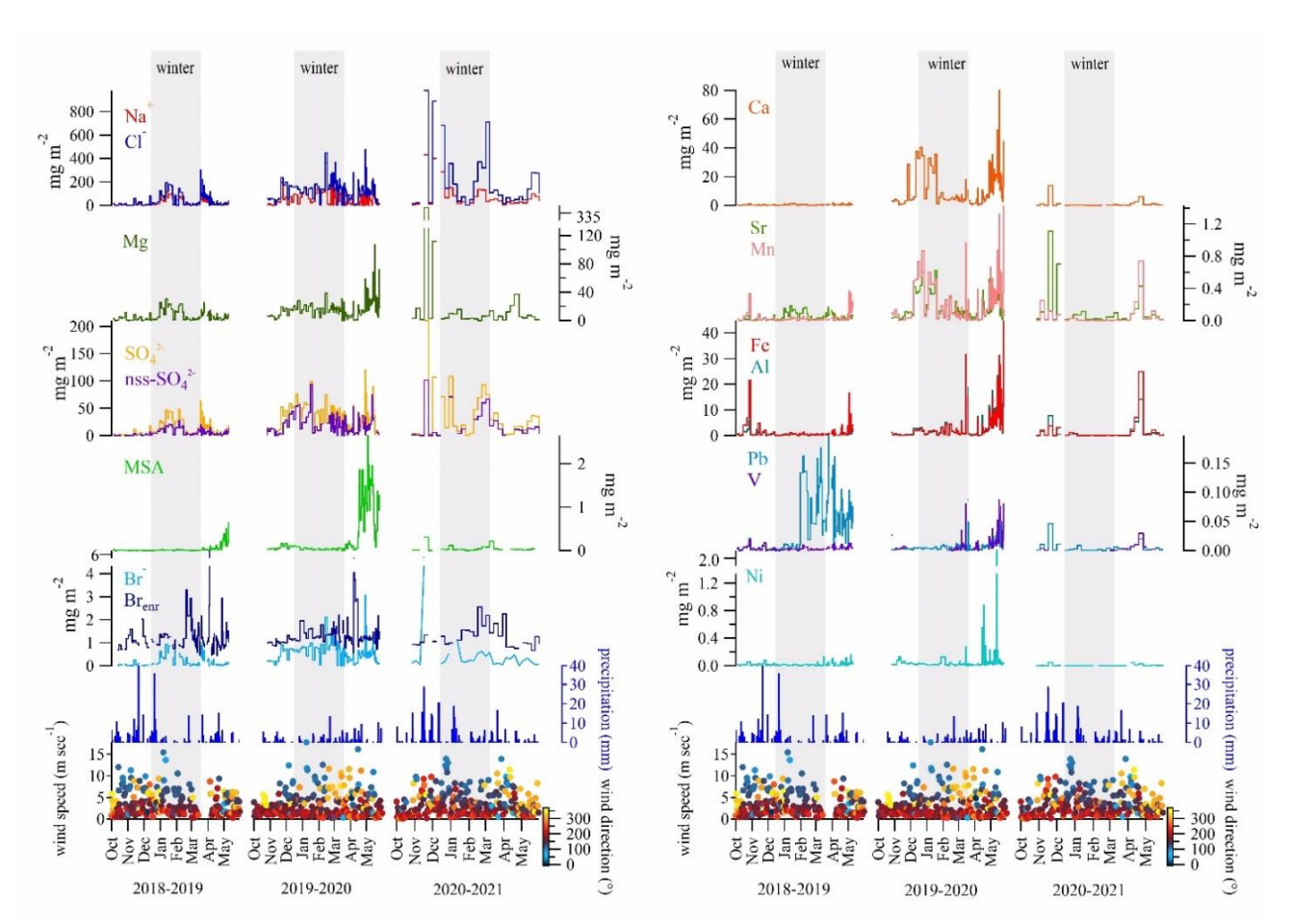


**Figure 2.** Wind direction (°), wind speed (m sec<sup>-1</sup>), and ionic loads (mg m<sup>-2</sup>) of Na<sup>+</sup>, Cl<sup>-</sup>, Mg, SO<sub>4</sub><sup>2-</sup>, nss-SO<sub>4</sub><sup>2-</sup>, MSA, Br<sup>-</sup>, Ca, Sr, Mn, Fe, Al, Pb, V, Ni in the surface snow for the three sampling campaigns: 2018-19, 2019-20, 2020-21. Seasonal trends are here presented for specific elements to provide a detailed view of how concentrations vary across distinct sampling periods.

A singular case is represented by Pb, which showed a 12.5-fold increase during winter-spring 2019 period compared to autumn 2018. The EF for Pb during these seasons exceeded 100, indicating a strong anthropogenic contribution. In contrast, the peak observed in 2020 no longer shows such elevated EF values (slightly above 10), suggesting a mixed source (Fig. 3). This implies that the April-May 2020 peak is largely of crustal origin, as the overlap with V (EF < 10) also suggests, possibly due to local dust events driven by strong winds exceeding the 5 m sec<sup>-1</sup> threshold (Fig. 2; Table S3).

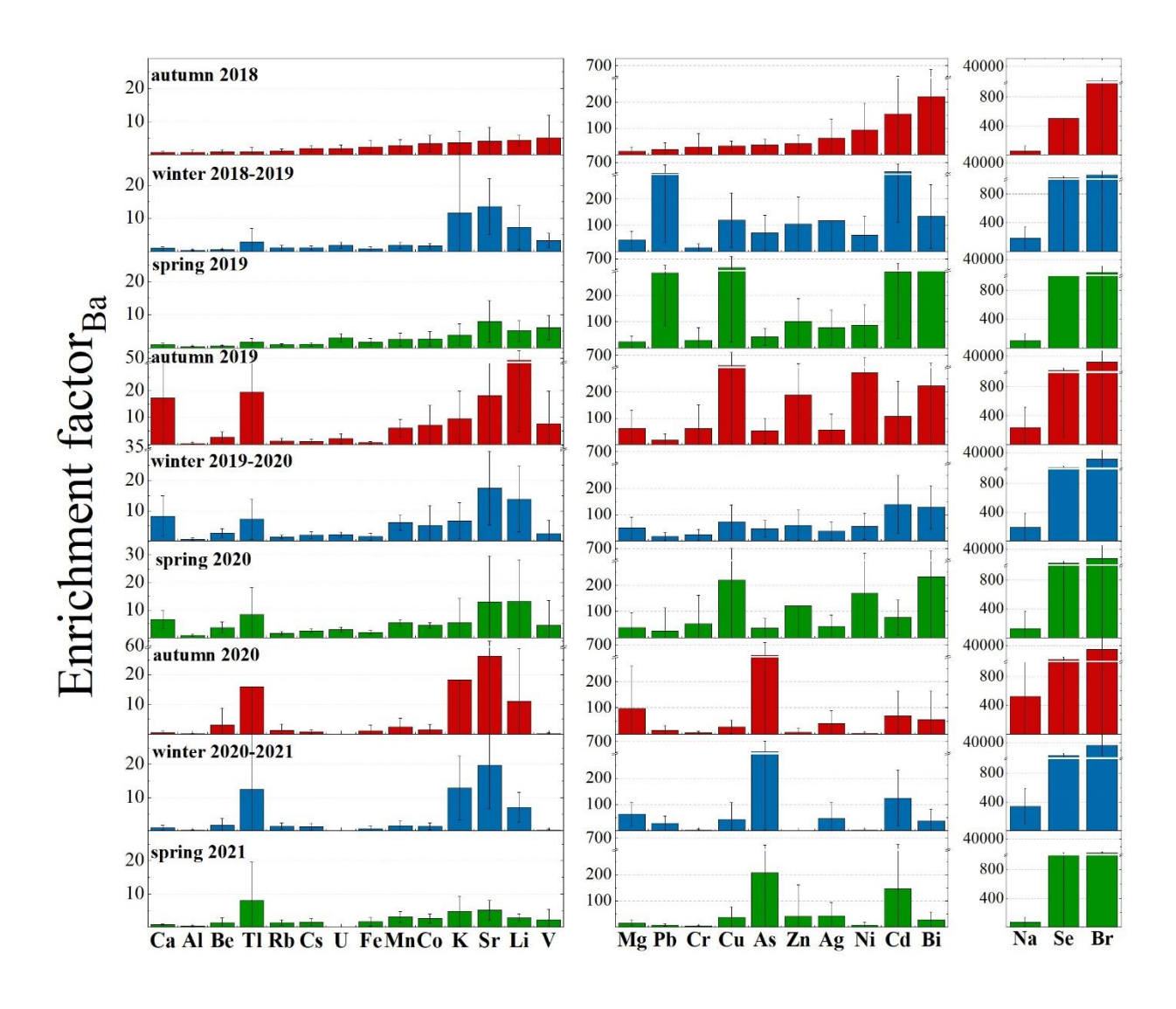


**Figure 3.** Enrichment Factors (EFs) calculated on all the presented trace elements for the three sampling campaigns: 2018-19, 2019-20, 2020-21. Calculating EFs for the full dataset offers a more robust assessment of potential sources and enrichment patterns, minimizing the variability inherent in individual seasons and allowing for a clearer distinction between crustal and non-crustal contributions.

The calculated EFs (Fig. 3) for Be, Al, V, Mn, Fe, Co, Rb, Cs, and U were consistently below 10, indicating a predominantly crustal (geogenic) origin for these elements. In contrast, Ni, and Sr displayed EFs greater than 10, suggesting contributions from mixed sources. Notably, Ni exhibited

exceptionally high EF values – above 100 – during autumn 2019 and spring 2020 (Ni). Mixed sources were also recognised for Li, K, Cr, Cu, Zn, As, Ag, Cd, and Tl with occasional EF values over 100. This suggests significant anthropogenic contributions, especially for Cu (spring and autumn 2019; spring 2020), As (from autumn 2020 to spring 2021), Zn (autumn 2019) and Cd (from autumn 2018 to spring 2019; winter 2019-20).

The 2019 springtime Pb concentration maxima are typically consistent with a mixture of eastern and western European sources (Sherrell et al., 2000; Bazzano et al., 2015, 2021). In this study, cluster mean trajectories obtained for winter 2018-2019 highlighted a 25% of air mass provenance from Russian Arctic and a 13% from eastern Siberia (Fig. S6), possibly explaining the higher concentrations of Pb revealed in spring 2019, following a reduced precipitation regime that occurred in January 2019. A local anthropogenic origin can be excluded though, since no activities (ordinary-extraordinary maintenance or particular events) were recorded in the vicinity of the sampling site in 2019. In addition, both GSRS and Ny-Ålesund (Fig. S2), located at 1 km of distance from each other, recorded comparable high concentrations of Pb, thus ruling out a possible contamination. However, at present, the long-range transport of Pb remains a hypothesis, likely supported by the breakdown of the wintry polar vortex (Fig. 1).

Backward trajectories (Fig. S6) for Ny-Ålesund area (78.92° N, 11.89° E) appear mostly in line with literature findings (Platt et al., 2022; Vecchiato et al., 2024), showing three main seasonal characters: a prevalent mass movement from ice-covered Central Arctic Ocean, Kara Sea, and Greenland Sea during autumn, a main provenance from Central Arctic Ocean and Kara Sea during winter, and a predominant trajectory from Northern Canada in addition to air masses arriving from Arctic Ocean and Kara seas during spring.

## 4.2 The main ion sources in the seasonal snow of Ny-Ålesund

Examining the dominant ions associated with marine aerosol, we found Cl<sup>-</sup>/Na<sup>+</sup> median ratios ranging from 1.3 to 1.5 w w<sup>-1</sup>, slightly lower than the expected value of 1.8 w w<sup>-1</sup> in the pure seawater (Zhuang et al., 1999), pointing the occurrence of a minimum Cl<sup>-</sup> depletion in aerosol, quantified as 14% for the 2018-19 and 2019-20 campaigns, and as just 2% for the 2020-21 campaign. A possible explanation for this phenomenon could be the de-chlorination of sea-spray aerosol during transport. This reaction occurs when sea-salt particles containing NaCl interact with acids such as HNO<sub>3</sub>, H<sub>2</sub>SO<sub>4</sub>, or organic acids, leading to the release of gaseous HCl (Zhuang et al., 1999, and reference therein). Although less likely, this process could also occur at the snow-atmosphere interface. On the

contrary, a possible influence of biomass burning on Cl<sup>-</sup> depletion process has been excluded by the very low correlation (0.18, p value < 0.05) found between Cl<sup>-</sup> depletion values and nss-K<sup>+</sup>/K<sup>+</sup> ratios, which is a tracer of relative contribution of biomass burning (Song et al., 2018).

441

442

443

444

445

446

447

448

449

450

451

452

453

454

455

456

457

458

459

460

461

462

463

464

465

466

467

468

469

470

Positive correlations between Mg, Ca, and K<sup>+</sup> with Na<sup>+</sup> and Cl<sup>-</sup> (all above 0.90, p value <0.05) suggest a common sea-spray source. However, the concentrations of Mg are also positively correlated with nss-Ca ( $\rho_{load} = 0.55$ ), calculated according to Morales et al. (1998), indicating a shared non-marine source. This suggests that in addition to their marine origin, these ions (Mg, Ca) also have contributions from a non-marine, crustal source. Further evidence comes from the Ca/Mg ratios in surface snow samples collected during the three campaigns, which were higher than those found in seawater (0.32, Millero et al., 2008). This excess indicates the likely presence of mineral particles (i.e., calcite and dolomite), potentially originating from local rock or soil dust (e.g., limestone, dolostone, and marble, which are abundant in Svalbard), as previously observed by Barbaro et al. (2021). To further explore the mixed sources of these elements, we calculated the Enrichment Factors (EFs) of Mg and Ca. For Mg, the EF values were consistently above 10 in all the seasons analysed, indicating a significant non-crustal source (e.g., marine). In contrast, Ca displayed EF values greater than 10 only during autumn 2019, suggesting that its non-crustal contribution (likely from sea spray) was more pronounced during that specific season. Based on these findings, we conclude that Mg and Ca effectively share a common sea spray origin, but the sea-salt contribution of Ca was mainly significant in autumn 2019, while the excess of Ca in other seasons likely reflects inputs from crustal source, such as local mineral dust.

Similarly, sulphate  $(SO_4^{2-})$  is highly and significantly correlated (p < 0.05) with both  $Na^+$  ( $\rho_{load} = 0.76$ ) and  $Cl^-$  ( $\rho_{load} = 0.93$ ), indicating that sea-spray is its main source. Nonetheless,  $Na^+/SO_4^{2-}$  and  $Cl^-/SO_4^{2-}$  ratios are significantly lower than typical seawater values (3.97 and 7.13, respectively, according to Millero et al., 2008) for the former two campaigns (2018-19, 2019-20). The elevated sulphate concentrations compared to sodium, also in winter snow, suggest the absence of a strong frost flower signature. Additionally, the lack of significant depletion in nss- $SO_4^{2-}$  further supports the minimal role of frost flowers in contributing to the snow composition. Therefore, while frost flowers are known to impact snow chemistry in Svalbard (Rankin et al., 2002; Beaudon and Moore, 2009; Roscoe et al., 2011), our analysis indicates that their contribution to the observed sea salt peaks in Kongsfjorden during the 2018-19, 2019-20 campaigns was likely limited. This analysis highlights that, while sea ice extent supports higher sea-salt concentrations in snow, the specific sulfate and ion ratios observed point to sea spray as the main source, with only a minor role for frost flower-related inputs.

- Instead, the presence of nss-SO<sub>4</sub><sup>2</sup>- suggests potential inputs from other sources, such as crustal
- material, anthropogenic emissions (e.g., fossil fuel combustion), or the oxidation of dimethylsulfide
- 473 (DMS) released from marine biological activities.
- To estimate the crustal fraction of sulphate (cr-SO<sub>4</sub><sup>2-</sup>), the nss-Ca (as crustal marker) content was
- multiplied by 0.59 (SO<sub>4</sub><sup>2</sup>-/Ca w/w ratio in the uppermost Earth crust Wagenbach et al. 1996),
- obtaining variable contributions for the three sampling campaigns, ranging from 2.45% up to 12.94%.
- Conversely, the anthropogenic contribution to nss-SO<sub>4</sub><sup>2-</sup> concentrations was investigated by the
- application of the [ex- SO<sub>4</sub><sup>2</sup>-] concentration formula (Schwikowski et al., 1999), considering the
- average concentration of [Ca] instead of the average ionic concentration [Ca<sup>2+</sup>] because Ca<sup>2+</sup>
- 480 concentrations were not measured in the samples collected during the second campaign due to
- 481 instrumental limitations:
- 482 [ex- $SO_4^{2-}$ ] =  $[SO_4^{2-}]$   $(0.12 [Na^+])$   $(0.175 [Ca^{2+}])$
- The obtained results showed a 50 up to 60% of anthropogenic contribution for the nss-SO<sub>4</sub><sup>2-</sup> input.
- 484 This finding corroborates previous results from Amore et al. (2022), who noted that anthropogenic
- sulphate was the most abundant apportioned component at Gruvebadet, accounting for at least 50%
- all over the year during the 2010-2019 investigated period. The plausible source of the anthropogenic
- fraction is the atmospheric transport of secondary aerosols containing  $SO_4^{2-}$ , and ammonium sulphate.
- 488 This sulphate can be formed by SO<sub>x</sub> emitted from coal combustion throughout the winter and biomass
- burning in the spring (Barbaro et al., 2021 and reference therein). The nss-SO<sub>4</sub><sup>2-</sup> does not correlate
- significantly with other ionic species (except for Mg), thus suggesting a separate origin.
- To quantify the biogenic nss-SO<sub>4</sub><sup>2</sup>- contribution, the methanesulfonic acid (MSA) loads the final
- 492 product of DMS oxidation were multiplied by 3.0 (Udisti et al., 2016), revealing biogenic SO<sub>4</sub><sup>2</sup>-
- 493 contributions ranging from 0.15% (2018-19, 2020-21) up to 0.38% (2019-20). Furthermore, the
- MSA/nss-SO<sub>4</sub><sup>2-</sup> ratio was inspected, revealing a mean value of  $0.02 \pm 0.03$  during the first (2018-19)
- and the third (2020-21) sampling campaigns, and a maximum ratio equal to  $0.06 \pm 0.18$  reached
- during the second campaign (2019-20), similar to the subarctic western North Pacific ratio found by
- Jung et al. (2014). However, several factors can influence MSA formation, a univocal marker of
- 498 biogenic emissions, including higher biological productivity related to higher nutrient input; the
- 499 concentrations of NO<sub>3</sub> radicals as key oxidants for DMS decomposition (higher NO<sub>3</sub> gives higher
- 500 MSA); and lower air temperatures, which tend to yield higher MSA levels (Andreae et al., 1985;
- 501 Udisti et al., 2020).

For the 2019-20 campaign, it seems likely that a combination of these three factors, together with the 502 positive expansion of sea ice and the very close drift ice presence in March 2020, as revealed from 503 satellite reconstructions (Fig. S7), contributed to the increased release of MSA in aerosol, and its 504 consistent deposition in surface snow (Fig. 2). Indeed, DMS was likely accumulated under the sea 505 ice cover in the fjord and surrounding areas, and then being released and oxidised in atmosphere when 506 the ice broke off and melted (April-May). Furthermore, lower temperatures, highly positive 507 correlation between MSA and  $NO_3^-$  ( $\rho_{load} = 0.64$ ), and high-speed short-range transport (wind 508 directions between  $0^{\circ}$ - $60^{\circ}$  and speeds > 5 m sec<sup>-1</sup>) from the source to the near-coast sink site (GSRS) 509 510 would have aided elevated concentrations of MSA in atmospheric depositions. However, the dominant south and southwest winds (180°-240°) during the major MSA peak in April 2020 (Fig. 2) 511 512 likely transported marine aerosols and DMS from open ocean regions, further facilitating the increased MSA concentrations observed. 513

- Contrarily, in the 2018-19 season, sea ice lasted only until April and was restricted to the inner, 514 shallower parts of Kongsfjorden (Assmy et al., 2023), possibly not allowing enough time with 515 adequate sunlight for substantial biological activity to accumulate beneath or within it. This occurred 516 despite the dominance in 2019, unlike the following year, of *Phaeocystis pouchetii*, a phytoplankton 517 518 species known for its capacity to generate DMS in significant quantities, according to Assmy et al. 519 (2023).
- Finally, the ammonium (NH<sub>4</sub><sup>+</sup>) load showed significant positive correlations with Na<sup>+</sup> ( $\rho_{load} = 0.76$ ), 520
- $Cl^{-}(\rho_{load} = 0.62)$  and  $K^{+}(\rho_{load} = 0.75)$ , as well as with  $SO_4^{2-}(\rho_{load} = 0.62)$ ,  $NO_3^{-}(\rho_{load} = 0.58)$ , MSA 521
- $(\rho_{load} = 0.52)$  and Br<sup>-</sup>  $(\rho_{load} = 0.62)$ , suggesting a close link with sea-salt ions and biogenic emissions. 522
- However, some contribution from biomass burning events and potential influence from 523
- 524 anthropogenic activities cannot be excluded.

#### 525 4.3 Bromine enrichment

- The bromine enrichment factor (Brenr) is well known to reflect specific processes (i.e., sea ice gas 526 phase Br emission) that affect the Br concentration and load in the snowpack (Spolaor et al., 2014). 527 Therefore, calculating the relative enrichment over the Br/Na ratio in sea water can offer crucial 528 529 insights on sea ice variability for the investigated Arctic areas (Barbaro et al., 2021). As reported in previous studies (Maffezzoli et al., 2017; Barbaro et al., 2021), the Br enrichment factor (Brenr) can 530 be calculated as  $Br_{enr} = Br^{-}/(0.0065 \text{ Na}^{+})$ , where 0.0065 represents the  $Br^{-}/Na^{+}$  seawater mass ratio. 531
- Contrarily to what observed in a former study (Barbaro et al., 2021) for the Hornsund area and north-532

western Spitsbergen, where the  $Br_{enr}$  mean values were often < 1, indicating some  $Br^-$  depletion, in this study we observed  $Br_{enr}$  mean values ranging from 1.5 up to 17.7, with the highest value associated to the second sampling campaign conducted in 2019-20, which showed the most extensive sea ice coverage. These results support the impact of the sea ice expansion and the close drift ice in the Kongsfjorden on the snow chemical composition. Indeed, newly formed sea ice releases gasphase Br into the polar atmosphere, thus supplying an extra  $Br^-$  source in addition to sea spray (Spolaor et al., 2016).

#### 4.3 Anthropogenic and natural sources of ions and particulate trace elements

533

534

535

536

537

538

539

540

541

542

543

544

545

546

547

548

549

550

551

552

553

554

555

556

557

558

559

560

561

To complement the EFs analysis and further distinguish possible anthropogenic contributions from natural ones (marine and geogenic) for ions and particulate trace elements, a Hierarchical Cluster Analysis (HCA) method was carried out. Results of clustering (Fig. 4) clearly disentangle marine (Na<sup>+</sup>, Cl<sup>-</sup>, K<sup>+</sup>, NH<sub>4</sub><sup>+</sup>, SO<sub>4</sub><sup>2-</sup>, NO<sub>3</sub><sup>-</sup>, Br<sup>-</sup>, Mg, Sr, bio-SO<sub>4</sub><sup>2-</sup>, MSA), anthropogenic (As, Co, Ag, Ba, Cd, Zn, Pb, Bi, Cr, Cu, Ni), and geogenic (nss-Ca, Tl, Li, Al, Cs, Rb, Fe, Mn, U, Be, Se, V) sources of ionic and elemental species, considering the whole sampling campaign period (2018-2021). Interestingly, nss-SO<sub>4</sub><sup>2-</sup> is brought together with the marine cluster, suggesting that its presence is largely influenced by marine biogenic sources, alongside contributions from secondary sulfate formation in the atmosphere. This indicates that nss-SO<sub>4</sub><sup>2</sup>, despite having a variety of sources such as human contribution or dust, is closely linked to the marine environment. One important reason for this is the emission of DMS by phytoplankton. Additionally, secondary sulfate formation may have further contributed to the nss-SO<sub>4</sub><sup>2</sup>-. Co was grouped within the anthropogenic cluster in HCA, in contrast with EFs that suggested a crustal origin. However, the errors associated with the EFs are quite high. Moreover, the trend for cobalt closely aligns with anthropogenic ones (e.g., As), while distinct trends are evident for crustal elements. Therefore, while the HCA results offer a reliable perspective on source differentiation and clustering patterns, they are best interpreted as complementary to the EF calculations rather than directly integrated with them. Incorporating EFs directly into the HCA could introduce significant inaccuracies, as EFs rely on reference element ratios that may vary and thus add complexity to the clustering process, potentially skewing the results. Consequently, HCA independently provides robust insights in this context, enhancing our understanding without the additional uncertainties that EF-based clustering might introduce.

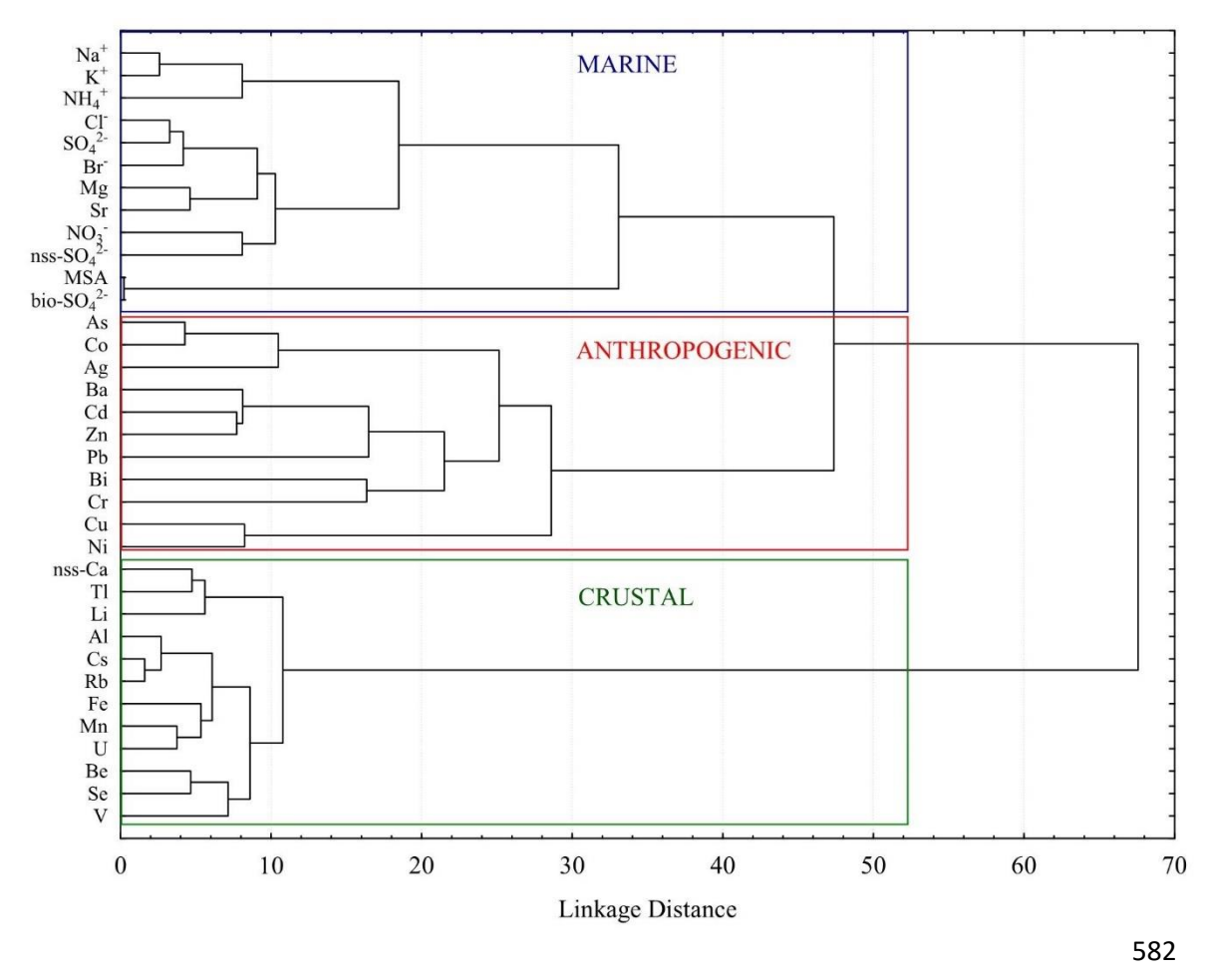


Figure 4. Hierarchical cluster analysis applied to further disentangle the particulate trace element non-crustal sources.

### 5. Summary and Conclusion

In this study, trace elements and major ions were investigated in surface snow samples collected in Ny-Ålesund between October 2018 to June 2021. Seasonal and interannual variations of impurities have been observed, with general higher concentrations of marine species revealed in late spring 2020, associated to more extensive sea ice in Kongsfjorden in March 2020, promoted by negative temperature anomalies in both atmosphere and ocean and likely related to higher air mass recycle within the Arctic. In fact, sea ice has a role in concentrating, storing, and releasing marine species, as well as influencing atmospheric and oceanic processes that affect their production and distribution. Higher concentrations in spring 2020 for geogenic and anthropogenic species were attributed instead to higher wind speeds, low atmospheric temperature anomalies, and generally drier conditions resulting from the exceptional occurrence of a strong and cold wintry stratospheric polar vortex, accompanied by an unprecedently positive phase of the Arctic Oscillation in the troposphere during January-March 2020. Therefore, our results highlighted a close dependence of high concentrations of impurities found in the snowpack at Ny-Ålesund on meteorological conditions, especially during cold

years, when the production of sea spray related aerosol likely derives by a larger extension of sea ice and stronger local Arctic circulation. The identification of geogenic, marine, and anthropogenic sources in the snowpack was allowed by a chemometric approach (HCA), which clarified the EFs results. The back trajectories analysis revealed distinct seasonal air mass patterns. During fall and winter, air mass predominantly originated from Northern Canada in addition to air masses arriving from Arctic Ocean and Kara seas during spring. On the contrary, no prevalent mid-latitude air currents were revealed in spring as expected, considering the period of the three sampling campaigns (2018-2021). These findings offer new insights into how specific meteorological and oceanic conditions, such as sea ice extent, wind speeds, and Arctic Oscillation phases, influence the chemical composition of the snowpack in Svalbard, particularly within the context of Arctic Amplification.

## Data availability

599

600

601

602

603

604

605

606

607

608

609

613

624

626

- The data supporting the findings of this study are available within the article and its supplementary
- 611 materials. Other data that support the findings of this study are available from the corresponding
- author upon request.

#### **Author contribution**

- 614 AS: Conceptualization, Data curation, Investigation, Writing-original draft, Writing-review and
- editing. EB: Conceptualization, Field work, Data curation, Formal Analysis, Writing-original draft,
- Writing-review and editing, Funding acquisition. MF: Formal Analysis, Field work, Data curation,
- Writing-review and editing. FS: Field work, Formal analysis, Investigation, Writing-review and
- editing. MV: Writing-review and editing. MV: Field work, Writing-review and editing. MM:
- 619 Investigation. FB: Investigation, Writing-review and editing. FB: Investigation. Field work. CJMH:
- 620 Investigation, Data curation, Writing-review and editing. AB: Field work, Data curation, Writing-
- review and editing. AG: Resources, Supervision, Validation, Writing-review and editing, Funding
- 622 acquisition. CB: Resources, Supervision, Validation, Writing-review and editing, Funding
- acquisition. AS: Funding acquisition, Supervision, Validation, Writing-review and editing.

#### **Competing interests**

The authors declare that they have no conflict of interest.

## Acknowledgments

- This project has received funding from the European Union's Horizon 2020 research and innovation 627
- programme under grant agreement no. 689443 via ERA\_PLANET Strand 4 project iCUPE 628
- (Integrative and Comprehensive Understanding on Polar Environments). We are grateful to the Arctic 629
- Station Dirigibile Italia from the Italian National Research Council Institute of Polar Science (CNR-630
- ISP) for logistical support. The authors gratefully acknowledge Claudio Artoni, Maria Papale, Ivan 631
- Sartorato, Federico Dallo, Alice Callegaro, Marco Casula, Mariasilvia Giamberini, Fabio Giardi, and 632
- all the station leaders of "Dirigibile Italia" who participated and offered valuable help and logistic 633
- support during the 2018-2021 sampling campaigns. Furthermore, we acknowledge Klara Wolf, Linda 634
- 635 Rehder, and Ane Kvernvik for help with CTD sampling. We acknowledge the help of ELGA
- LabWater in providing the PURELAB Pulse and PURELAB Flex, which produced the ultrapure 636
- water used in these experiments. 637

#### References

638

- Amore, A., Giardi, F., Becagli, S., Caiazzo, L., Mazzola, M., Severi, M., Traversi, R.: Source 639 640 apportionment of sulphate in the High Arctic by a 10 yr-long record from Gruvebadet Observatory
- Atmos. 118890. (Ny-Ålesund. Svalbard Islands). Environ., 270. 1-10. 641
- https://doi.org/10.1016/j.atmosenv.2021.118890, 2022 642
- Andreae, M.O., Ferek, R.J., Bermond, F., Byrd, K.P., Engstrom, R.T., Hardin, S., Houmere, 644
- P.D., LeMarrec, F., Raemdonck, H., Chatfield, R.B.: Dimethyl sulfide in the marine atmosphere, 645
- J. Geophys. Res., 90, D7, 12891-12900, https://doi.org/10.1029/JD090iD07p12891, 1985 646
- Assmy, P., Kvernvik, A.C., Hop, H., Hoppe, C.J.M., Chierici, M., David, D., Duarte, P., 647
- Fransson, A., Garcia, L.M., Patuła, W., Kwaśniewski, S., Maturilli, M., Pavlova, O., Tatarek, A., 648
- Wiktor, J.M., Wold, A., Wolf, K.K.E., Bailey, A.: Seasonal plankton dynamics in Kongsfjorden 649
- during two years of contrasting environmental conditions, Prog. Oceanogr., 213, 102996, 650
- https://doi.org/10.1016/j.pocean.2023.102996, 2023 651
- 652 Barbaro, E., Koziol, K., Björkman, M.P., Vega, C.P., Zdanowicz, C., Martma, T., Gallet, J.C.,
- Kępski, D., Larose, C., Luks, B., Tolle, F., Schuler, T. V., Uszczyk, A., Spolaor, A.: Measurement 653
- report: Spatial variations in ionic chemistry and water-stable isotopes in the snowpack on glaciers 654
- across Svalbard during the 2015-2016 snow accumulation season, Atmos. Chem. Phys., 21, 3163-655
- 656 3180, https://doi.org/10.5194/acp-21-3163-2021, 2021
- Barbaro, E., Padoan, S., Kirchgeorg, T., Zangrando, R., Toscano, G., Barbante, C., Gambaro, 657
- A.: Particle size distribution of inorganic and organic ions in coastal and inland Antarctic aerosol, 658
- Environ. Sci. Pollut. Res., 24, 2724-2733, https://doi.org/10.1007/s11356-016-8042-x, 2017 659
- 660 Barbaro, E., Zangrando, R., Vecchiato, M., Piazza, R., Cairns, W.R.L., Capodaglio, G.,
- Barbante, C., Gambaro, A.: Free amino acids in Antarctic aerosol: Potential markers for the evolution 661
- and fate of marine aerosol, Atmos. Chem. Phys., 15, 5457-5469, https://doi.org/10.5194/acp-15-662
- 5457-2015, 2015 663

- Bazzano, A., Ardini, F., Becagli, S., Traversi, R., Udisti, R., Cappelletti, D., Grotti, M.: Source assessment of atmospheric lead measured at Ny-Ålesund, Svalbard, Atmos. Environ., 113, 20-26, https://doi.org/10.1016/j.atmosenv.2015.04.053, 2015
- Bazzano, A., Bertinetti, S., Ardini, F., Cappelletti, D., Grotti, M.: Potential Source Areas for
- https://doi.org/10.3390/atmos12030388, 2021

668

Beaudon, E., Moore, J.: Frost flower chemical signature in winter snow on Vestfonna ice cap,

atmospheric Lead reaching Ny-Ålesund from 2010 to 2018, Atmos., 12, 388, 1-17,

- Nordaustlandet, Svalbard, Cryosphere, 3, 147–154, https://doi.org/10.5194/tc-3-147-2009, 2009
- Beine, H.J., Dominé, F., Ianniello, A., Nardino, M., Allegrini, I., Teinilä, K., Hillamo, R.:
- Fluxes of nitrates between snow surfaces and the atmosphere in the European high Arctic, Atmos.
- 674 Chem. Phys., 3, 335-346, https://doi.org/10.5194/acp-3-335-2003, 2003
- Bertò, M., Cappelletti, D., Barbaro, E., Varin, C., Gallet, J.-C., Markowicz, K.,
- 676 Rozwadowska, A., Mazzola, M., Crocchianti, S., Poto, L., Laj, P., Barbante, C., Spolaor, A.:
- Variability in black carbon mass concentration in surface snow at Svalbard, Atmos. Chem. Phys., 21,
- 678 12479-12493, https://doi.org/10.5194/acp-21-12479-2021, 2021
- Björkman, M., Kühnel, R., Partridge, D.G., Roberts, T.J., Aas, W., Mazzola, M., Viola, A.,
- 680 Hodson, A., Ström, J., Isaksson, E.: Nitrate dry deposition in Svalbard, Tellus B, 65(1),
- 681 https://doi.org/10.3402/tellusb.v65i0.19071, 2013
- Chylek, P., Folland, C., Klett, J.D., Wang, M., Hengartner, N., Lesins, G., Dubey, M.K.:
- Annual Mean Arctic Amplification 1970-2020. Observed and Simulated by CMIP6 Climate Models,
- Geophys. Res. Lett., 49 (13), e2022GL099371, https://doi.org/10.1029/2022GL099371, 2022
- D'Amico, M., Kallenborn, R., Scoto, F., Gambaro, A., Gallet, J.-C., Spolaor, A., Vecchiato,
- 686 M.: Chemicals of Emerging Arctic Concern in north-western Spitsbergen snow: Distribution and
- sources, Sci. Total Environ., 908, 168401, https://doi.org/10.1016/j.scitotenv.2023.168401, 2024
- Dethloff, K., Maslowski, W., Hendricks, S., Lee, Y.J., Goessling, H.F., Krumpen, T., Haas,
- 689 C., Handorf, D., Ricker, R., Bessnov, V., Cassano, J.J., Kinney, J.C., Osinski, R., Rex, M., Rinke, A.,
- 690 Sokolova, J., Sommerfeld, A.: Arctic sea ice anomalies during the MOSAiC winter 2019/20,
- 691 Cryosphere, 16, 981-1005, https://doi.org/10.5194/tc-16-981-2022, 2022
- Draxler, R.R.: An overview of the HYSPLIT\_4 modelling system for trajectories, dispersion
- 693 and deposition, Aust. Meteorol. Mag., 47, 295–308, 1998
- Eleftheriadis, K., Vratolis, S., Nyeki, S.: Aerosol black carbon in the European Arctic:
- Measurements at Zeppelin station, Ny-Ålesund, Svalbard from 1998-2007, Geophys. Res. Lett., 36,
- 696 1–5, https://doi.org/10.1029/2008GL035741, 2009
- Feltracco, M., Barbaro, E., Hoppe, C.J.M., Wolf, K.K.E., Spolaor, A., Layton, R., Keuschnig,
- 698 C., Barbante, C., Gambaro, A., Larose, C.: Airborne bacteria and particulate chemistry capture
- 699 Phytoplankton bloom dynamics in an Arctic fjord, Atmos. Environ., 256, 118458.
- 700 https://doi.org/10.1016/j.atmosenv.2021.118458, 2021
- Feltracco, M., Barbaro, E., Tedeschi, S., Spolaor, A., Turetta, C., Vecchiato, M., Morabito,
- 702 E., Zangrando, R., Barbante, C., Gambaro, A.: Interannual variability of sugars in Arctic aerosol:
- 703 Biomass burning and biogenic inputs, Sci. Total Environ., 706, 136089,
- 704 https://doi.org/10.1016/j.scitotenv.2019.136089, 2020

- Geng, H., Ryu, J., Jung, H.J., Chung, H., Ahn, K.H.O., Ro, C.U.N.: Single-particle characterization of summertime arctic aerosols collected at Ny-Ålesund, Svalbard, Environ. Sci. Technol., 44, 2348–2353, https://doi.org/10.1021/es903268j, 2010
- George, B.J., Gains-Germain, L., Broms, K., Black, K., Furman, M., Hays, M.D., Thomas, K.W., Simmons, J.E.: Censoring trace-level environmental data: statistical analysis considerations to limit bias, Environ. Sci. Technol., 55(6), 3786-3795, https://doi.org/10.1021/acs.est.0c02256, 2021
- Gerland, S., Pavlova, O., Marnela, M., Divine, D.V., Kohler, J., Renner, A., Skoglund, A.: Sea ice extent variability in Kongsfjorden, Svalbard during 2003-2021, based on visual observations from the mountain Zeppelinfjellet, Norwegian Polar Institute, https://doi.org/10.21334/npolar.2022.d6d31f5b, 2022
- Gjermundsen, A., Seland Graff, L., Bentsen, M., Anders Breivik, L., Boldingh Debernard, J., Makkonen, R., Olivié, D.J.L., Seland, Ø., Zieger, P., Schulz, M.: How representative is Svalbard for future Arctic climate evolution? An Earth system modelling perspective (SvalCLIM), SESS Report 2020 – The State of Environmental Science in Svalbard, https://doi.org/10.5281/zenodo.4034104,
- 719 2020
- Hansen, B.B., Isaksen, K., Benestad, R.E., Kohler, J., Pedersen, Å., Loe, L.E., Coulson, S.J., Larsen, J.O., Varpe, Ø.: Warmer and wetter winters: Characteristics and implications of an extreme weather event in the High Arctic, Environ. Res. Lett., 9, https://doi.org/10.1088/1748-9326/9/11/114021, 2014
- Hodgkins, R., Tranter, M.: Solute in High Arctic glacier snow cover and its impact on runoff chemistry, Ann. Glaciol., 26, 156-160, https://doi.org/10.3189/1998AoG26-1-156-160, 1998
- Jacobi, H.-W., Obleitner, F., Da Costa, S., Ginot, P., Eleftheriadis, K., Aas, W., Zanatta, M.:
  Deposition of ionic species and black carbon to the Arctic snowpack: combining snow pit
  observations with modeling, Atmos. Chem. Phys., 19, 10361-10377,
  https://doi.org/10.3402/tellusb.v65i0.19071, 2019
- Jung, J., Furutani, H., Uematsu, M., Park, J.: Distributions of atmospheric non-sea-salt sulphate and methanesulfonic acid over the Pacific Ocean between 48°N and 55°S during summer, Atmos. Environ., 99, 374-384, https://doi.org/10.1016/j.atmosenv.2014.10.009, 2014
- Koziol, K., Uszczyk, A., Pawlak, F., Frankowski, M., Polkowska, Ż.: Seasonal and Spatial Differences in Metal and Metalloid Concentrations in the Snow Cover of Hansbreen, Svalbard, Front. Earth Sci., 8, 1–8, https://doi.org/10.3389/feart.2020.538762, 2021
- Lai, A.M., Shafer, M.M., Dibb, J.E., Polashenski, C.M., Schauer, J.J.: Elements and inorganic ions as source tracers in recent Greenland snow, Atmos. Environ., 164, 205–215, https://doi.org/10.1016/j.atmosenv.2017.05.048, 2017
- Lawrence, Z.D., Perlwitz, J., Butler, A.H., Manney, G.L., Newman, P.A., Lee, S.H., Nash, E.R.: The Remarkably Strong Arctic Stratospheric Polar Vortex of Winter 2020: Links to Record-Breaking Arctic Oscillation and Ozone Loss, J. Geophys. Res. Atmos., 125, 1–21, https://doi.org/10.1029/2020JD033271, 2020
- Maffezzoli, N., Spolaor, A., Barbante, C., Bertò, M., Frezzotti, M., Vallelonga, P.: Bromine,
- iodine and sodium in surface snow along the 2013 Talos Dome-GV7 traverse (northern Victoria Land, East Antarctica), Cryosphere, 11, 693-705, https://doi.org/10.5194/tc-11-693-2017, 2017

- Millero, F.J., Feistel, R., Wright, D.G., McDougall, T.J.: The composition of Standard Seawater and the definition of the Reference-Composition Salinity Scale, Deep-Sea Res., 55, 50–72,
- 748 2008
- Morales, J.A., Pirela, D., de Nava, M.G., de Borrego, B.S., Velásquez, H., Durán, J.: Inorganic
- vater soluble ions in atmospheric particles over Maracaibo Lake Basin in the western region of
- 751 Venezuela, Atmos. Res., 46, https://doi.org/10.1016/S0169-8095(97)00071-9, 1998
- Nawrot, A.P., Migała, K., Luks, B., Pakszys, P., Głowacki, P.: Chemistry of snow cover and
- acidic snowfall during a season with a high level of air pollution on the Hans Glacier, Spitsbergen,
- 754 Polar Sci., 10, 249–261, https://doi.org/10.1016/j.polar.2016.06.003, 2016
- Platt, S.M., Hov, Ø., Berg, T., Breivik, K., Eckhardt, S., Eleftheriadis, K., Evangeliou, N.,
- Fiebig, M., Fisher, R., Hansen, G., Hansson, H.-C., Heintzenberg, J., Hermansen, O., Heslin-Rees,
- 757 D., Holmén, K., Hudson, S., Kallenborn, R., Krejci, R., Krognes, T., Larssen, S., Lowry, D., Lund
- 758 Myhre, C., Lunder, C., Nisbet, E., Nizzetto, P.B., Park, K.-T., Pedersen, C.A., Pfaffhuber, K.A.,
- Röckmann, T., Schmidbauer, N., Solberg, S., Stohl, A., Ström, J., Svendby, T., Tunved, P., Tørnkvist,
- 760 K., van der Veen, C., Vratolis, S., Yoon, Y.L., Yttri, K.E., Zieger, P., Aas, W., Tørseth, K.:
- 761 Atmospheric composition in the European Arctic and 30 years of the Zeppelin Observatory, Ny-
- <sup>762</sup> Ålesund, Atmos. Chem. Phys., 22, 3321-3369, https://doi.org/10.5194/acp-22-3321-2022, 2022
- Pomeroy, J.W.: A process-based model of snow drifting, Ann. Glaciol., 13, 237-240,
- 764 https://doi.org/10.3189/S0260305500007965, 1989
- Rankin, A.M., Wolff, E.W.: Frost flowers: Implications for tropospheric chemistry and ice
- core interpretation, J. Geophys. Res., 107, D23, 4683, https://doi.org/10.1029/2002JD002492, 2002
- Rantanen, M., Karpechko, A.Y., Lipponen, A., Nordling, K., Hyvärinen, O., Ruosteenoja, K.,
- Vihma, T., Laaksonen, A.: The Arctic has warmed nearly four times faster than the globe since 1979,
- 769 Commun. Earth Environ, 3, 168, https://doi.org/10.1038/s43247-022-00498-3, 2022
- Rinke, A., Maturilli, M., Graham, R.M., Matthes, H., Handorf, D., Cohen, L., Hudson, S.R.,
- Moore, J.C.: Extreme cyclone events in the Arctic: Wintertime variability and trends, Environ. Res.
- 772 Lett., 12, https://doi.org/10.1088/1748-9326/aa7def, 2017
- Roscoe, H.K., Brooks, B., Jackson, A.V., Smith, M.H., Walker, S.J., Obbard, R.W., Wolff,
- E.W.: Frost flowers in the laboratory: Growth, characteristics, aerosol, and the underlying sea ice, J.
- 775 Geophys. Res., 116, D12301, https://doi.org/10.1029/2010JD015144, 2011
- Ruppel, M.M., Khedr, M., Liu, X., Beaudon, E., Szidat, S., Tunved, P., Ström, J., Koponen,
- H., Sippula, O., Isaksson, E., Gallet, J.-C., Hermanson, M., Manninen, S., Schnelle-Kreis, J.: Organic
- compounds, radiocarbon, trace elements and atmospheric transport illuminating sources of elemental
- 779 carbon in a 300-year Svalbard ice core, J. Geophys. Res.: Atmos., 128,
- 780 https://doi.org/10.1029/2022JD038378, 2023
- Salzano, R., Cerrato, R., Scoto, F., Spolaor, A., Valentini, E., Salvadore, M., Esposito, G.,
- 782 Sapio, S., Taramelli, A., Salvatori, R.: Detection of winter heat wave impact on surface runoff in a
- 783 periglacial environment (Ny-Ålesund, Svalbard), Remote Sens., 15(18), 4435,
- 784 https://doi.org/10.3390/rs15184435, 2023

- Schoeberl, M.R., Newman, P.A.: Middle Atmosphere: Polar Vortex, Encyclopedia of Atmospheric Sciences, Second Edition, Elsevier, 12-17, https://doi.org/10.1016/B978-0-12-382225-3.00228-0, 2015
- Schwikowski, M., Döscher, A., Gäggeler, H.W., Schotterer, U.: Anthropogenic versus natural sources of atmospheric sulphate from an Alpine ice core. Tellus B: Chemical and Physical Meteorology, 51:5, 938-951, https://doi.org/10.3402/tellusb.v51i5.16506, 1999
- Scoto, F., Pappaccogli, G., Mazzola, M., Donateo, A., Salzano, R., Monzali, M., de Blasi, F., 791 792 Larose, C., Gallet, J.-C., Decesari, S., Spolaor, A.: Automated observation of physical snowpack 793 properties in Ny-Ålesund, Front. Earth Sci., 11:1123981, 1-9, https://doi.org/ 0.3389/feart.2023.1123981, 2023 794
- Serreze, M.C., Barry, R.G.: Processes and impacts of Arctic amplification: A research synthesis, Glob. Planet. Change, 77, 85-96, http://dx.doi.org/10.1016/j.gloplacha.2011.03.004, 2011
- Sherrell, R.M., Boyle, E.A., Harris, N.R., Falkner, K.K.: Temporal variability of Cd, Pb, and Pb isotope deposition in central Greenland snow, Geochem Geophys, 1 (1), 1-22, https://doi.org/10.1029/1999GC000007, 2000
- Sobota, I., Weckwerth, P., Grajewski, T.: Rain-On-Snow (ROS) events and their relations to snowpack and ice layer changes on small glaciers in Svalbard, the high Arctic, J. Hydrol, 590, 125279, https://doi.org/10.1016/j.jhydrol.2020.125279, 2020
- Song, C., Becagli, S., Beddows, D.C.S., Brean, J., Browse, J., Dai, Q., Dall'Osto, M., Ferracci, V., Harrison, R.M., Harris, N., Li, W., Jones, A.E., Kirchgäßner, A., Kramawijaya, A.G., Kurganskiy, A., Lupi, A., Mazzola, M., Severi, M., Traversi, R., Shi, Z.: Understanding sources and drivers of size-resolved aerosol in the High Arctic islands of Svalbard using a receptor model coupled with machine learning, Environ. Sci. Technol., 56, 11189-11198, https://doi.org/10.1021/acs.est.1c07796, 2022
- Song, J., Zhao, Y., Zhang, Y., Fu, P., Zheng, L., Yuan, Q., Wang, S., Huang, X., Xu, W., Cao, Z., Gromov, S., Lai, S.: Investigation of biomass burning on atmospheric aerosols over the western South China Sea: Insights from ions, carbonaceous fractions and stable carbon isotope ratios, Environ. Pollut., 242, 1800-1809, https://doi.org/10.1016/j.envpol.2018.07.088, 2018
- Spolaor, A., Scoto, F., Larose, C., Barbaro, E., Burgay, F., Bjorkman, M., Cappelletti, D., Dallo, F., de Blasi, F., Divine, D., Dreossi, G., Gabrieli, J., Isaksson, E., Kohler, J., Martma, T., Schmidt, L.S., Schuler, T.V., Stenni, B., Turetta, C., Luks, B., Casado, M., Gallet, J.-C.: Climate change is rapidly deteriorating the climatic signal in Svalbard glaciers, Cryosphere, 18, 307-320,
- 817 https://doi.org/10.5194/tc-18-307-2024, 2024
- Spolaor, A., Varin, C., Pedeli, X., Christille, J.M., Kirchgeorg, T., Giardi, F., Cappelletti, D., Turetta, C., Cairns, W.R.L., Gambaro, A., Bernagozzi, A., Gallet, J.C., Björkman, M.P., Barbaro, E.: Source, timing and dynamics of ionic species mobility in the Svalbard annual snowpack, Sci. Total Environ., 751, 141640, https://doi.org/10.1016/j.scitotenv.2020.141640, 2021b
- Spolaor, A., Moroni, B., Luks, B., Nawrot, A., Roman, M., Larose, C., Stachnik, Ł., Bruschi, F., Kozioł, K., Pawlak, F., Turetta, C., Barbaro, E., Gallet, J.-C., Cappelletti, D.: Investigation on the Sources and Impact of Trace Elements in the Annual Snowpack and the Firn in the Hansbreen (Southwest Spitsbergen), Front. Earth Sci., 8, 1–10, https://doi.org/10.3389/feart.2020.536036, 2021a

- Spolaor, A., Barbaro, E., Cappelletti, D., Turetta, C., Mazzola, M., Giardi, F., Björkman, M.P.,
- 827 Lucchetta, F., Dallo, F., Aspmo Pfaffhuber, K., Angot, H., Dommergue, A., Maturilli, M., Saiz-
- 828 Lopez, A., Barbante, C., Cairns, W.R.L.: Diurnal cycle of iodine, bromine, and mercury
- 829 concentrations in Svalbard surface snow, Atmos. Chem. Phys., 19, 13325-13339,
- 830 https://doi.org/10.5194/acp-19-13325-2019, 2019
- Spolaor, A., Angot, H., Roman, M., Dommergue, A., Scarchilli, C., Vardè, M., Del Guasta,
- 832 M., Pedeli, X., Varin, C., Sprovieri, F., Magand, O., Legrand, M., Barbante, C., Cairns, W.R.L:
- Feedback mechanisms between snow and atmospheric mercury: Results and observations from field
- 834 campaigns on the Antarctic plateau, Chemosphere, 197, 306–317,
- https://doi.org/10.1016/j.chemosphere.2017.12.180, 2018
- Spolaor, A., Opel, T., McConnell, J.R., Maselli, O.J., Spreen, G., Varin, C., Kirchgeorg, T.,
- 837 Fritzsche, D., Saiz-Lopez, A., Vallelonga, P.: Halogen-based reconstruction of Russian Arctic sea ice
- 838 area from the Akedemii Nauk ice core (Severnaya Zemlya), Cryosphere, 10, 245-256,
- 839 https://doi.org/10.5194/tc-10-245-2016, 2016
- Spolaor, A., Vallelonga, P., Gabrieli, J., Martma, T., Björkman, M.P., Isaksson, E., Cozzi, G.,
- Turetta, C., Kjær, H.A., Curran, M.A.J., Moy, A.D., Schönhardt, A., Blechschmidt, A.-M., Burrows,
- J.P., Plane, J.M.C., Barbante, C.: Seasonality of halogen deposition in polar snow and ice, Atmos.
- 843 Chem. Phys., 14, 18, 9613-9622, https://doi.org/10.5194/acp-14-9613-2014, 2014
- Stein, A.F., Draxler, R.R., Rolph, G.D., Stunder, B.J.B., Cohen, M.D., Ngan, F.: Noaa's
- hysplit atmospheric transport and dispersion modeling system, Bull. Am. Meteorol. Soc., 96, 2059–
- 846 2077, https://doi.org/10.1175/BAMS-D-14-00110.1, 2015
- Stohl, A., Berg, T., Burkhart, J.F., Fjæraa, a. M., Forster, C., Herber, A., Hov, Ø., Lunder, C.,
- McMillan, W.W., Oltmans, S., Shiobara, M., Simpson, D., Solberg, S., Stebel, K., Ström, J., Tørseth,
- 849 K., Treffeisen, R., Virkkunen, K., Yttri, K.E.: Arctic smoke record high air pollution levels in the
- 850 European Arctic due to agricultural fires in Eastern Europe, Atmos. Chem. Phys. Discuss., 6, 9655–
- 851 9722, https://doi.org/10.5194/acpd-6-9655-2006, 2006b
- Stohl, A., Berg, T., Burkhart, J.F., Fjæraa, a. M., Forster, C., Herber, A., Hov, Ø., Lunder, C.,
- McMillan, W.W., Oltmans, S., Shiobara, M., Simpson, D., Solberg, S., Stebel, K., Ström, J., Tørseth,
- 854 K., Treffeisen, R., Virkkunen, K., Yttri, K.E.: Arctic smoke record high air pollution levels in the
- 855 European Arctic due to agricultural fires in Eastern Europe, Atmos. Chem. Phys. Discuss., 6, 9655–
- 856 9722, https://doi.org/10.5194/acpd-6-9655-2006, 2006a
- Turetta, C., Feltracco, M., Barbaro, E., Spolaor, A., Barbante, C., Gambaro, A.: A year-round
- 858 measurement of water-soluble trace and rare earth elements in arctic aerosol: Possible inorganic
- tracers of specific events, Atmosphere, 12, https://doi.org/10.3390/atmos12060694, 2021
- Udisti, R., Traversi, R., Becagli, S., Tomasi, C., Mazzola, M., Lupi, A., Quinn, P.K.: Arctic
- Aerosols, in: Physics and Chemistry of the Arctic Atmosphere, Springer Polar Sciences, edited by:
- 862 Kokhanovsky, A., Tomasi, C., 209-329, https://doi.org/10.1007/978-3-030-33566-3\_4, 2020
- Udisti, R., Bazzano, A., Becagli, S., Bolzacchini, E., Caiazzo, L., Cappelletti, D., Ferrero, L.,
- 864 Frosini, D., Giardi, F., Grotti, M., Lupi, A., Malandrino, M., Mazzola, M., Moroni, B., Severi, M.,
- Traversi, R., Viola, A., Vitale, V.: Sulphate source apportionment in the Ny-Ålesund (Svalbard
- 866 Islands) Arctic aerosol, Rend. Fis. Acc. Lincei, 27, Suppl 1: S85-S94, https://doi.org/10.1007/s12210-
- 867 016-0517-7, 2016

- Vecchiato, M., Barbante, C., Barbaro, E., Burgay, F., Cairns, W.R.L., Callegaro, A.,
- 869 Cappelletti, D., Dallo, F., D'Amico, M., Feltracco, M., Gallet J.-C., Gambaro, A., Larose, C.,
- 870 Maffezzoli, N., Mazzola, M., Sartorato, I., Scoto, F., Turetta, C., Vardè, M., Xie, Z., Spolaor, A.: The
- 871 seasonal change of PAHs in Svalbard surface snow, Environ. Pollut., 340, 122864,
- 872 https://doi.org/10.1016/j.envpol.2023.122864, 2024
- Vecchiato, M., Barbaro, E., Spolaor, A., Burgay, F., Barbante, C., Piazza, R., Gambaro, A.:
- Fragrances and PAHs in snow and seawater of Ny-Ålesund (Svalbard): Loca and long-range
- contamination, Environ. Pollut., 242, 1740-1747, https://doi.org/10.1016/j.envpol.2018.07.095, 2018
- Vega, C.P., Björkman, M.P., Pohjola, V.A., Isaksson, E., Pettersson, R., Martma, T., Marca,
- A., Kaiser, J., Vega, C.P., Björkman, M.P., Pohjola, V.A., Isaksson, E., Pettersson, R., Martma, T.,
- Marca, A., Kaiser, J., Pohjola, V.A., Isaksson, E., Pettersson, R., Vega, C.P., Bjo, M.P.: Nitrate stable
- 879 isotopes and major ions in snow and ice samples from four Svalbard sites Nitrate stable isotopes and
- major ions in snow and ice samples from four Svalbard sites, Polar Res., 2015, 34, 23246,
- 881 https://doi.org/10.3402/polar.v34.23246, 2015
- Wagenbach, D., Preunkert, S., Schäfer, J., Jung, W., Tomadin, L.: Northward transport of
- 883 Saharan dust recorded in a deep alpine ice core, in: The impact of desert dust across the
- mediterranean, Springer, The Netherlands, edited by: Guerzoni, S., Chester, R., 291-300, 1996
- Wedepohl, K.H.: The composition of the chemical crust. Geoch. Cosm. Act., 59(7), 1217-
- 886 1232, https://doi.org/10.1016/0016-7037(95)00038-2, 1995
- Yttri, K.E., Lund Myhre, C., Eckhardt, S., Fiebig, M., Dye, C., Hirdman, D., Ström, J.,
- Klimont, Z., Stohl, A.: Quantifying black carbon from biomass burning by means of levoglucosan -
- A one-year time series at the Arctic observatory Zeppelin, Atmos. Chem. Phys., 14, 6427–6442,
- 890 https://doi.org/10.5194/acp-14-6427-2014, 2014a
- Zhan, J., Gao, Y., Li, W., Chen, L., Lin, H., Lin, Q.: Effects of ship emissions on summertime
- 892 aerosols at Ny-Alesund in the Arctic, Atmos. Pollut. Res., 5, 500-510,
- 893 https://doi.org/10.5094/APR.2014.059, 2014

896

- Zhuang, H., Chan, C.K., Fang, M., Wexler, A.S.: Size distributions of particulate sulphate,
- nitrate, and ammonium at a coastal site in Hong Kong, Atmos. Environ., 33, 843-853, 1999